

## Gain recovery time in a terahertz quantum cascade laser

David R. Bacon, Joshua R. Freeman,<sup>a)</sup> Reshma A. Mohandas, Lianhe Li, Edmund H. Linfield, A. Giles Davies, and Paul Dean

*School of Electronic and Electrical Engineering, University of Leeds, Woodhouse Lane, Leeds LS9 2JT, United Kingdom*

(Received 7 October 2015; accepted 8 February 2016; published online 22 February 2016)

The gain recovery time of a bound-to-continuum terahertz frequency quantum cascade laser, operating at 1.98 THz, has been measured using broadband terahertz-pump-terahertz-probe spectroscopy. The recovery time is found to reduce as a function of current density, attaining a value of 18 ps as the laser is brought close to threshold. We attribute this reduction to improved coupling efficiency between the injector state and the upper lasing level as the active region aligns. © 2016 Author(s). All article content, except where otherwise noted, is licensed under a Creative Commons Attribution 3.0 Unported License. [<http://dx.doi.org/10.1063/1.4942452>]

The development of quantum cascade lasers (QCLs) in the terahertz (THz) frequency region of the spectrum has seen significant progress in recent years.<sup>1</sup> Amongst other achievements, these devices have now been demonstrated to operate up to 200 K (Ref. 2) and emit output powers up to 1 W.<sup>3</sup> These features, coupled with their compact size and narrow emission linewidth, have led to applications in imaging<sup>4</sup> and gas sensing.<sup>5</sup>

There has also been significant interest in understanding emission from QCLs in the time-domain, and the generation of pulses on ultrafast timescales. The integration of THz-QCLs with time-domain spectroscopy (TDS)<sup>6–8</sup> techniques has allowed the measurement of the electric field of the laser emission with an extremely high time resolution. This has revealed a complex time-domain pulse structure, even when the QCL is operated at a fixed current.<sup>9</sup> At the same time, active modelocking has also been developed. Coherent measurements have been reported using both an electrical feedback technique<sup>10</sup> and a technique based on THz pulse injection seeding of a QCL.<sup>11</sup> This research has highlighted the instabilities present in QCL emission<sup>12</sup> and the difficulty of forming stable modelocked pulses from this type of device owing to the interplay of the inherent characteristic lifetimes. In fact, there are several lifetimes that are important in determining the characteristics of the laser emission, including the dephasing time of the laser transition, the photon lifetime, the cavity round trip time, and the gain recovery time (GRT). In many lasing systems, these lifetimes will be significantly different, leading to predictable dynamics. In QCLs, however, they are expected to have similar values, in the range of 1–50 ps, with the value of the GRT being least well established. Crucially, it is the ratio between the GRT and the round-trip time of the laser cavity that is important for achieving modelocking; if the GRT is short compared with the round trip time, then the gain will recover before a pulse circulating in the cavity returns to the same point, enabling several pulses to propagate simultaneously and thus preventing the onset of modelocking.

There has been one experimental measurement of the GRT in THz QCLs till date.<sup>13</sup> This work did not, however, measure gain directly, but rather the recovery of photocurrent as a function of time delay between two high-power THz pulses, generated by a free-electron laser. A value of 50 ps for the GRT was found, which is significantly longer than the 2–3 ps measured for mid-infrared (mid-IR) frequency QCLs<sup>14,15</sup> using an IR pump-probe technique. The GRT has also been inferred indirectly from simulations of pulse-seeding in THz QCLs; this enabled an estimate of the GRT to be made of around 15 ps.<sup>16</sup> In our work, we measure the GRT of a bound-to-continuum THz QCL, similar to the device used in Ref. 13, directly, using a THz-pump-THz-probe technique. The GRT of the THz QCL is a function of bias and is found to reduce as the device approaches threshold, at which point a value of 18 ps is obtained.

The experiment was conducted using the arrangement shown in Fig. 1. The system is based on a femtosecond laser, centered at 800 nm, providing 100 fs pulses at an 80 MHz repetition rate and 2 W average power. The beam was first split, and the more powerful (90%) component was further

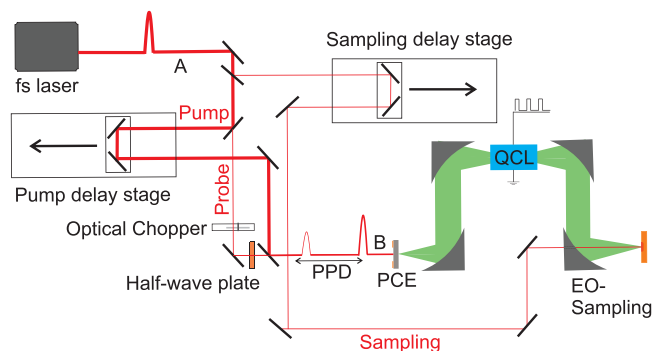


FIG. 1. THz-TDS arrangement adapted for pump-probe measurements of a THz-QCL. At point A, the average optical power is measured to be 2.0 W. Three beam-splitters are shown, two of which have 90:10 splitting ratios and are used to separate the original pulse into pump, probe, and sampling pulses. The pump and probe pulses are recombined at the third beam-splitter, providing a total average optical power at point B of 1.1 W. The pump and probe are perpendicularly polarized to each other. The pump-probe delay is abbreviated to “PPD,” the photoconductive emitter to “PCE,” and electro-optic to “EO.”

<sup>a)</sup>Electronic mail: j.r.freeman@leeds.ac.uk

divided into “pump” and “probe.” The pump beam, with an average power of approximately 1 W, passed through a delay stage, allowing independent variation in arrival times of the pump and probe signals. The probe beam, with an average power of 100 mW, passed through a half-wave plate and an optical chopper, to discriminate between the pump and probe signals. The half-wave plate was set to ensure the pump and probe beams had orthogonal polarization; this reduced any interference effects between the near-IR pulses incident on the emitter. The probe beam was then recombined with the pump beam after a delay stage and focused onto a photoconductive emitter; this had a large-area antenna with a 100  $\mu\text{m}$  gap that was fabricated on a 2  $\mu\text{m}$  thick low-temperature grown gallium arsenide (LT-GaAs) and biased at 110 V. For large-area emitters the dependence of the THz power on the incident polarization is weak, and the resulting linear THz polarization depends only on the electrode geometry. A hyper-hemispherical silicon lens was attached to the back of the emitter to increase the detected far-field signal, as well as to limit surface reflections. A weaker 20 mW “sampling” beam formed at the first beam splitter was steered through a second variable delay-stage before being used for electro-optic signal detection using a 2 mm thick ZnTe crystal.

Before introducing the QCL into the experiment, the response of the LT-GaAs emitter to the probe beam was measured as a function of pump-probe delay (PPD). Because of the depletion of carriers due to the initial pump pulse, the THz probe signal was found to reduce for small PPDs.<sup>17</sup> Nevertheless, we observed a fast recovery of the LT-GaAs emitter (of around 0.4 ps), and so, this effect is not expected to affect our experiments adversely since the smallest PPD used in this work was 2.5 ps. We also measured a slight increase in probe signal as the PPD decreases, but with a longer characteristic time-scale; we have normalized for this effect in the following work.

The QCL device used in this study was based on a GaAs/AlGaAs bound-to-continuum active region design,<sup>18</sup> processed into a 4.4 mm-long and 200  $\mu\text{m}$ -wide ridge, and confined with a vertical surface plasmon waveguide. The device was indium soldered to a copper mount and cooled to 15 K in a helium flow cryostat (Janis model ST-100). The threshold current density was found to be approximately 124 A/cm<sup>2</sup> and Fourier transform IR spectrometer (FTIR) data revealed single mode lasing at 1.98 THz. The QCL was positioned as shown in Fig. 1, and the broadband THz pulses, with polarization parallel to the growth direction, were coupled into the QCL facet using two off-axis parabolic mirrors. The THz “pump beam” arrives first at the QCL input facet, causing stimulated emission from the population inversion within the active region, depleting the population inversion and available gain. At a later time, the THz probe pulse enters the cavity and experiences amplification proportional to the population inversion in the active region. The probe pulse is then collected and measured by electro-optic sampling. The use of a long laser cavity in this work enhanced the reduction in population inversion because of the amplification of the pump pulse through the cavity. For cases where the probe pulse is weaker than the pump, calculations based on the Frantz-Nodvik equation<sup>19</sup> (1) show that the use of a long amplifier for these measurements can lead to a slight

over-estimation of the GRT. This effect is offset, however, when the effect of the pump reflection from the end facet of the cavity is taken into account, which acts to reduce the measured value of the GRT. For the present case (pump-probe power ratio of approximately five, and facet reflectivity of 0.3), we calculate that our measurements underestimate the underlying GRT by approximately 10%, when both of these effects are considered. This estimated correction factor has not been applied to the following results.

The QCL was driven by a square wave with frequency 3.8 kHz and 20% duty cycle (52.6  $\mu\text{s}$  pulse width). The emitter bias was synchronized to the second harmonic of this signal at 7.6 kHz, also with a 52.6  $\mu\text{s}$  pulse width. A lock-in amplifier referenced to the QCL bias was used to monitor the signal from the balanced photodiodes such that it measured the difference signal between the QCL on and off states, thereby removing spurious signals, such as those arising from pulses not travelling through the QCL.

Figure 2 shows the signal obtained with the probe beam blocked and the QCL biased below threshold at a current density of 114 A/cm<sup>2</sup>. In this case, the signal corresponds to the pump pulse following relative amplification in the QCL cavity. The bias of the LT-GaAs emitter was then varied so that the dependence of this amplification on input THz power could be determined. The input power was estimated from the signal FFT at 2 THz, measured when the QCL was unbiased. These results, shown in the lower inset, reveal that the pump pulse is partly able to saturate the population inversion. This data has been fitted to the Frantz-Nodvik equation

$$E_{\text{out}} = E_{\text{sat}} \ln \left[ e^{\frac{E_T}{E_{\text{sat}}}} \left( e^{\frac{E_{\text{in}}}{E_{\text{sat}}}} - 1 \right) + 1 \right], \quad (1)$$

where  $E_{\text{in}}$  is the pulse energy input,  $E_{\text{sat}}$  is the saturation energy,  $E_T$  is the total energy available from the amplifier, and  $E_{\text{out}}$  is the pulse energy output. To improve the quality of the fit, we have fixed the small-signal single-pass net gain to be equal to the loss from one mirror. This is a valid assumption because the device is operated just below

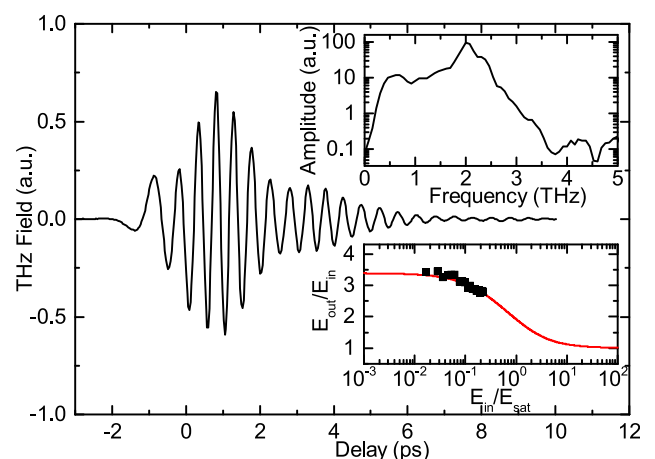


FIG. 2. Time-domain measurement of a broadband pulse, after passing through the QCL biased just below threshold. The upper inset shows an FFT of this time-domain signal. The lower inset shows the relationship between QCL cavity gain ( $E_{\text{out}}/E_{\text{in}}$ ) and injected pulse power (black squares).  $E_{\text{out}}$  and  $E_{\text{in}}$  have been measured from the FFT power at 2 THz and a fit based on the Frantz-Nodvik equation has also been plotted (red line). The x-axis has been scaled by the saturation energy,  $E_{\text{sat}}$ .

threshold. By considering Eq. (1) in the small-signal limit and using a facet reflectivity of  $R=0.3$ , we fix the small-signal single-pass net gain to be  $g_0 = \alpha_m = 2.7 \text{ cm}^{-1}$ , equivalent to  $E_T = 1.22E_{\text{sat}}$ . The fitting, with just one free parameter,  $E_{\text{sat}}$ , suggests that the maximum pump pulse energy injected into the cavity corresponds to  $E_{\text{in}} = 0.22E_{\text{sat}}$ . Using this information it is possible to estimate the saturation energy,  $E_{\text{sat}}$ , by estimating  $E_{\text{in}}$ . The pump power measured before the QCL is  $23 \mu\text{W}$ . This is multiplied by factors for the spectral overlap (0.14), mode-matching (0.3), facet transmission (0.7), and divided by the laser repetition rate (80 MHz) to estimate the pump pulse energy coupled into the QCL as 8.5 fJ. Using the relation found above, this gives  $E_{\text{sat}} \sim 38 \text{ fJ}$ .

In order to determine the GRT of the QCL, the probe pulse was measured for different time-delays with respect to the earlier pump pulse. To retrieve the probe signal, the output from the first lock-in amplifier (referenced to the QCL) was connected to a second lock-in amplifier, which was referenced to the optical chopper (shown in Figure 1) operating at 30 Hz. The modulation frequency for the second lock-in amplifier was limited by the need to be slow with respect to the time-constant of the first lock-in amplifier (which was set to 20 ms). In this way, the second lock-in amplifier was used to discriminate between the THz pump and THz probe signals so that only signals from the THz probe were measured. The QCL was again operated below threshold at  $121 \text{ A/cm}^2$ . Fig. 3(a) illustrates the probe signal for various PPD times, normalized to the peak of the incident THz probe pulse. As the PPD reduces, so does the relative gain at 2 THz, since the gain has less time to recover after the passage of the pump pulse. In the time-domain, this is indicated by the reduction in oscillation time and amplitude, while the spectra (Fig. 3(b)) reveal a reduced peak at 2 THz. Fig. 3(c) shows the peak spectral power at 2 THz as a function of PPD. This has been plotted for four separate bias conditions. Exponential fits have been used to determine the recovery time for these values of current density, and these are plotted together with the

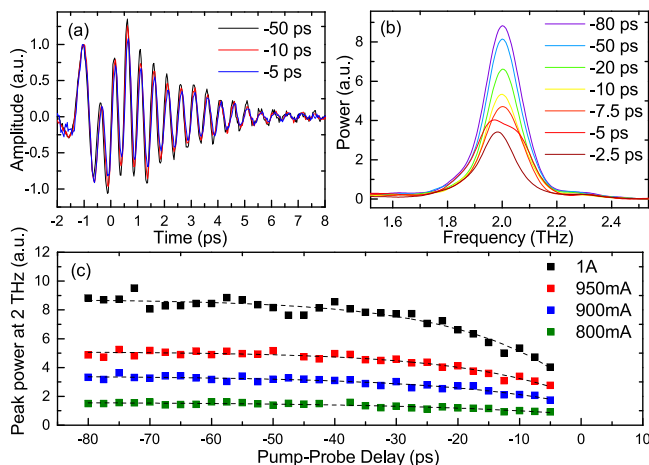


FIG. 3. (a) Time-domain trace of the probe pulse for various PPD times, normalised to the peak of the initial broadband THz pulse. (b) Frequency spectrum of the probe pulse for different PPD times. (c) Peak of the probe spectrum at the QCL emission frequency of 2 THz, as a function of PPD, plotted for four different QCL current-densities (squares). An exponential fit has been applied to each curve (black lines).

light-current-voltage characteristics for this device in Fig. 4. The data reveal a significant decrease in the GRT from 27 ps to 18 ps as the laser approaches threshold. The reduction in error bars as the QCL is brought closer to threshold is caused by the increased gain (and therefore signal) as the structure becomes more aligned. The mechanisms for gain recovery in this case can be divided into two sources, carrier transport out of the lower laser level through the extractor mini-band and carrier transport into the upper laser, through the “injection barrier” of the QCL (the thickest barrier in the active region period, immediately up-stream from the upper laser level). Miniband extraction is known to be dominated by rapid electron-electron scattering<sup>20</sup> on sub-ps time-scales that we are not able to resolve in this experiment. We therefore expect the recovery time observed to be dominated by carrier transport from the injector into the upper-lasing state. While we have not been able to perform quantitative calculations on carrier transfer rates, simple bandstructure calculations, based on a self-consistent Poisson-Schrodinger model, show that the injector-upper laser level coupling increases as the design is brought closer to full alignment.

As the QCL current is increased above threshold the mechanisms involved in gain recovery become more complex. The rise in the cavity photon density adds an additional mechanism for depopulation of the upper lasing level through stimulated emission. This mechanism is influenced by mirror losses, spectral hole burning, and the precise photon distribution in the cavity. For the purposes of rate equation calculations and modelocking considerations, only the “bare cavity,” purely electronic, recovery time is relevant. Typically, in pump-probe experiments, an apparent decrease in the upper-lasing state lifetime is measured above threshold.<sup>14</sup> Here, when operating the QCL above threshold, we observed an increased noise level and an increase in the extracted GRT values. This additional noise above threshold may be due to spatial and temporal variations of the THz laser field inside the cavity, which are known to form coherent instabilities.<sup>12</sup> While the average gain of the device is clamped, the cavity gain will not be temporally stable nor spatially uniform, and these variations would be sampled using our technique, leading to increased noise in our measurements. To obtain reliable measurements of the gain

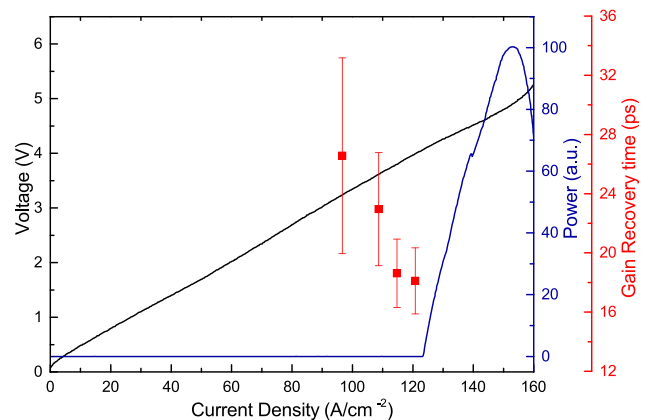


FIG. 4. Measured gain recovery time at different current densities (red squares), with error bars determined by the exponential fit. The blue line is the THz power measured with a pyroelectric detector. The black curve is the IV response of the QCL.

recovery time when the laser is biased for peak gain, anti-reflective coatings could be used to suppress lasing and move the threshold to higher current density. We also note that the rate of gain recovery is expected to differ for different active region designs, in particular, THz QCLs based on LO-phonon extraction (rather than the miniband extraction design measured here) are expected to exhibit faster dynamics and further measurements are required to investigate this.

In conclusion, we have shown that the GRT of a bound-to-continuum THz QCL is reduced as the laser is brought towards threshold, attaining a value of 18 ps just before laser action commences. This value is significantly higher than has been measured for QCLs operating in the mid-IR range (2–3 ps) where the active region transport is based on rapid phonon-depopulation designs. The values that we find are also significantly lower than those obtained by Green *et al.*,<sup>13</sup> where the photo-current through the QCL structure was measured; this may represent a recovery time for the device (rather than the laser transition) and hence be an upper limit for the GRT. We also note that the values we measure here agree well with the estimate of 15 ps obtained by Maxwell-Bloch simulations of pulsed seeding of a bound-to-continuum THz QCL.<sup>16</sup> The fast gain recovery measured in this work explains why conventional methods for modelocking THz QCLs are problematic. Given that the cavity round-trip time is generally 50–100 ps for most devices, THz QCLs will tend to support multiple pulses in the same cavity. Solutions to this problem include engineering active regions with longer recovery times<sup>21</sup> and more exotic modelocking methods.<sup>22</sup>

This work was supported by the Engineering and Physical Sciences Research Council [EP/J002356/1 and ‘COTS’, EP/J017671/1]. Support via the Royal Society Wolfson Research Merit Award Scheme (WM110032 and WM150029) is also acknowledged.

<sup>1</sup>B. S. Williams, *Nat. Photonics* **1**, 517 (2007).

<sup>2</sup>S. Fatholouloumi, E. Dupont, C. Chan, Z. Wasilewski, S. Laframboise, D. Ban, A. Mátyás, C. Jirascsek, Q. Hu, and H. Liu, *Opt. Express* **20**, 3866 (2012).

- <sup>3</sup>L. Li, L. Chen, J. Zhu, J. Freeman, P. Dean, A. Valavanis, A. G. Davies, and E. H. Linfield, *Electron. Lett.* **50**, 309 (2014).
- <sup>4</sup>P. Dean, A. Valavanis, J. Keeley, K. Bertling, Y. Lim, R. Alhathloul, A. Burnett, L. Li, S. Khanna, D. Indjin *et al.*, *J. Phys. D: Appl. Phys.* **47**, 374008 (2014).
- <sup>5</sup>H.-W. Hübers, S. Pavlov, H. Richter, A. Semenov, L. Mahler, A. Tredicucci, H. Beere, and D. Ritchie, *Appl. Phys. Lett.* **89**, 061115 (2006).
- <sup>6</sup>J. Kröll, J. Darmo, S. S. Dhillon, X. Marcadet, M. Calligaro, C. Sirtori, and K. Unterrainer, *Nature* **449**, 698 (2007).
- <sup>7</sup>N. Jukam, S. S. Dhillon, D. Oustinov, J. Madéo, C. Manquest, S. Barbieri, C. Sirtori, S. P. Khanna, E. H. Linfield, A. G. Davies *et al.*, *Nat. Photonics* **3**, 715 (2009).
- <sup>8</sup>D. Oustinov, N. Jukam, R. Rungsawang, J. Madéo, S. Barbieri, P. Filloux, C. Sirtori, X. Marcadet, J. Tignon, and S. Dhillon, *Nat. Commun.* **1**, 69 (2010).
- <sup>9</sup>J. Maysonave, N. Jukam, M. Ibrahim, K. Maussang, J. Madéo, P. Cavalié, P. Dean, S. P. Khanna, D. Steenson, E. H. Linfield *et al.*, *Opt. Lett.* **37**, 731 (2012).
- <sup>10</sup>S. Barbieri, M. Ravaro, P. Gellie, G. Santarelli, C. Manquest, C. Sirtori, S. P. Khanna, E. H. Linfield, and A. G. Davies, *Nat. Photonics* **5**, 306 (2011).
- <sup>11</sup>J. R. Freeman, J. Maysonave, N. Jukam, P. Cavalié, K. Maussang, H. E. Beere, D. A. Ritchie, J. Mangeney, S. S. Dhillon, and J. Tignon, *Appl. Phys. Lett.* **101**, 181115 (2012).
- <sup>12</sup>A. Gordon, C. Y. Wang, L. Diehl, F. X. Kärtner, A. Belyanin, D. Bour, S. Corzine, G. Höfler, H. C. Liu, H. Schneider, T. Maier, M. Troccoli, J. Faist, and F. Capasso, *Phys. Rev. A* **77**, 053804 (2008).
- <sup>13</sup>R. P. Green, A. Tredicucci, N. Q. Vinh, B. Murdin, C. Pidgeon, H. E. Beere, and D. A. Ritchie, *Phys. Rev. B* **80**, 075303 (2009).
- <sup>14</sup>H. Choi, L. Diehl, Z.-K. Wu, M. Giovannini, J. Faist, F. Capasso, and T. B. Norris, *Phys. Rev. Lett.* **100**, 167401 (2008).
- <sup>15</sup>W. Kuehn, W. Parz, P. Gaal, K. Reimann, M. Woerner, T. Elsaesser, T. Müller, J. Darmo, K. Unterrainer, M. Austerer *et al.*, *Appl. Phys. Lett.* **93**, 151106 (2008).
- <sup>16</sup>J. R. Freeman, J. Maysonave, S. Khanna, E. H. Linfield, A. G. Davies, S. S. Dhillon, and J. Tignon, *Phys. Rev. A* **87**, 063817 (2013).
- <sup>17</sup>M. Tonouchi, N. Kawasaki, T. Yoshimura, H. Wald, and P. Seidel, *Jpn. J. Appl. Phys., Part 2* **41**, L706 (2002).
- <sup>18</sup>J. R. Freeman, O. Marshall, H. E. Beere, and D. A. Ritchie, *Appl. Phys. Lett.* **93**, 191119 (2008).
- <sup>19</sup>L. M. Frantz and J. S. Nodvik, *J. Appl. Phys.* **34**, 2346 (1963).
- <sup>20</sup>R. Köhler, R. C. Iotti, A. Tredicucci, and F. Rossi, *Appl. Phys. Lett.* **79**, 3920 (2001).
- <sup>21</sup>C. Y. Wang, L. Kuznetsova, V. M. Gkortsas, L. Diehl, F. X. Kärtner, M. A. Belkin, A. Belyanin, X. Li, D. Ham, H. Schneider *et al.*, *Opt. Express* **17**, 12929 (2009).
- <sup>22</sup>C. R. Menyuk and M. A. Talukder, *Phys. Rev. Lett.* **102**, 023903 (2009).